

Welcome to [E-XFL.COM](https://www.e-xfl.com)

Understanding [Embedded - FPGAs \(Field Programmable Gate Array\)](#)

Embedded - FPGAs, or Field Programmable Gate Arrays, are advanced integrated circuits that offer unparalleled flexibility and performance for digital systems. Unlike traditional fixed-function logic devices, FPGAs can be programmed and reprogrammed to execute a wide array of logical operations, enabling customized functionality tailored to specific applications. This reprogrammability allows developers to iterate designs quickly and implement complex functions without the need for custom hardware.

Applications of Embedded - FPGAs

The versatility of Embedded - FPGAs makes them indispensable in numerous fields. In telecommunications.

Details

Product Status	Active
Number of LABs/CLBs	-
Number of Logic Elements/Cells	-
Total RAM Bits	276480
Number of I/O	223
Number of Gates	1500000
Voltage - Supply	1.425V ~ 1.575V
Mounting Type	Surface Mount
Operating Temperature	-55°C ~ 100°C (TJ)
Package / Case	484-BGA
Supplier Device Package	484-FPBGA (23x23)
Purchase URL	https://www.e-xfl.com/product-detail/microchip-technology/afs1500-1fgg484k

Instant On

Flash-based Fusion devices are Level 0 Instant On. Instant On Fusion devices greatly simplify total system design and reduce total system cost by eliminating the need for CPLDs. The Fusion Instant On clocking (PLLs) replaces off-chip clocking resources. The Fusion mix of Instant On clocking and analog resources makes these devices an excellent choice for both system supervisor and system management functions. Instant On from a single 3.3 V source enables Fusion devices to initiate, control, and monitor multiple voltage supplies while also providing system clocks. In addition, glitches and brownouts in system power will not corrupt the Fusion device flash configuration. Unlike SRAM-based FPGAs, the device will not have to be reloaded when system power is restored. This enables reduction or complete removal of expensive voltage monitor and brownout detection devices from the PCB design. Flash-based Fusion devices simplify total system design and reduce cost and design risk, while increasing system reliability.

Firm Errors

Firm errors occur most commonly when high-energy neutrons, generated in the upper atmosphere, strike a configuration cell of an SRAM FPGA. The energy of the collision can change the state of the configuration cell and thus change the logic, routing, or I/O behavior in an unpredictable way. Another source of radiation-induced firm errors is alpha particles. For an alpha to cause a soft or firm error, its source must be in very close proximity to the affected circuit. The alpha source must be in the package molding compound or in the die itself. While low-alpha molding compounds are being used increasingly, this helps reduce but does not entirely eliminate alpha-induced firm errors.

Firm errors are impossible to prevent in SRAM FPGAs. The consequence of this type of error can be a complete system failure. Firm errors do not occur in Fusion flash-based FPGAs. Once it is programmed, the flash cell configuration element of Fusion FPGAs cannot be altered by high-energy neutrons and is therefore immune to errors from them.

Recoverable (or soft) errors occur in the user data SRAMs of all FPGA devices. These can easily be mitigated by using error detection and correction (EDAC) circuitry built into the FPGA fabric.

Low Power

Flash-based Fusion devices exhibit power characteristics similar to those of an ASIC, making them an ideal choice for power-sensitive applications. With Fusion devices, there is no power-on current surge and no high current transition, both of which occur on many FPGAs.

Fusion devices also have low dynamic power consumption and support both low power standby mode and very low power sleep mode, offering further power savings.

Advanced Flash Technology

The Fusion family offers many benefits, including nonvolatility and reprogrammability through an advanced flash-based, 130-nm LVCMOS process with seven layers of metal. Standard CMOS design techniques are used to implement logic and control functions. The combination of fine granularity, enhanced flexible routing resources, and abundant flash switches allows very high logic utilization (much higher than competing SRAM technologies) without compromising device routability or performance. Logic functions within the device are interconnected through a four-level routing hierarchy.

Advanced Architecture

The proprietary Fusion architecture provides granularity comparable to standard-cell ASICs. The Fusion device consists of several distinct and programmable architectural features, including the following (Figure 1-1 on page 1-5):

- Embedded memories
 - Flash memory blocks
 - FlashROM
 - SRAM and FIFO

Last Known State – I/O is set to the last value that was driven out prior to entering the programming mode, and then held at that value during programming

Z -Tristate: I/O is tristated

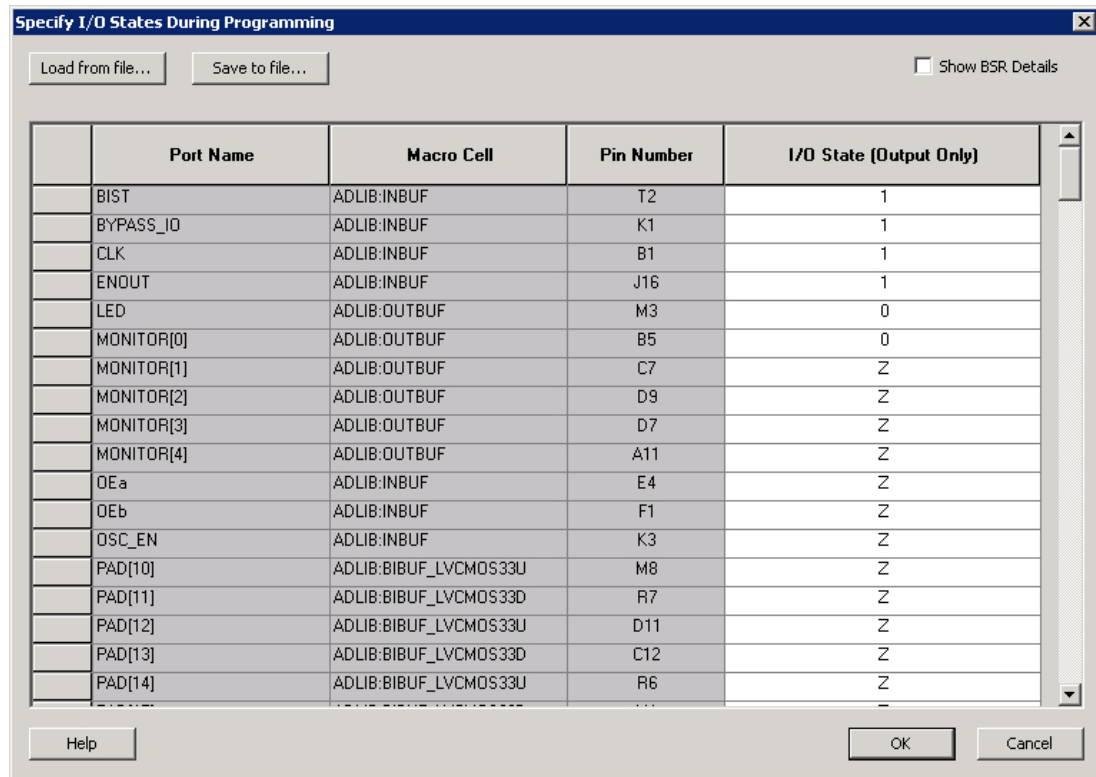


Figure 1-3 • I/O States During Programming Window

- Click **OK** to return to the FlashPoint – Programming File Generator window.

Note: I/O States During programming are saved to the ADB and resulting programming files after completing programming file generation.

VersaTile Characteristics

Sample VersaTile Specifications—Combinatorial Module

The Fusion library offers all combinations of LUT-3 combinatorial functions. In this section, timing characteristics are presented for a sample of the library (Figure 2-3). For more details, refer to the *IGLOO, ProASIC3, SmartFusion, and Fusion Macro Library Guide*.

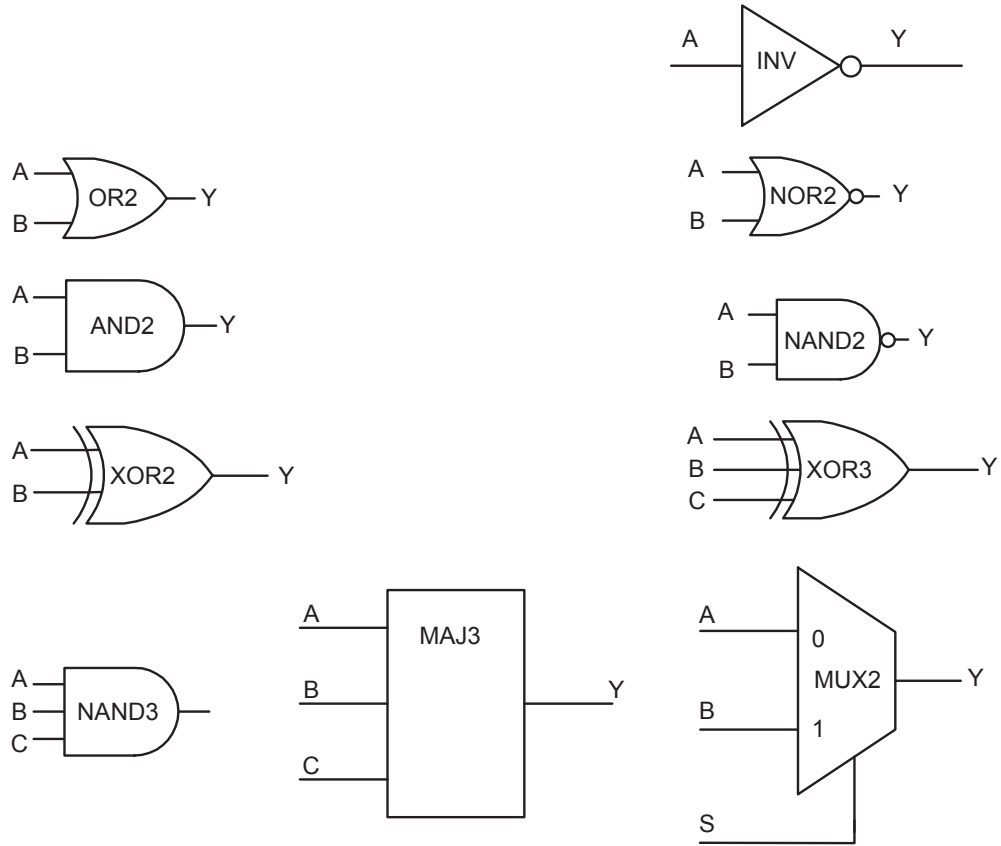


Figure 2-3 • Sample of Combinatorial Cells

Routing Architecture

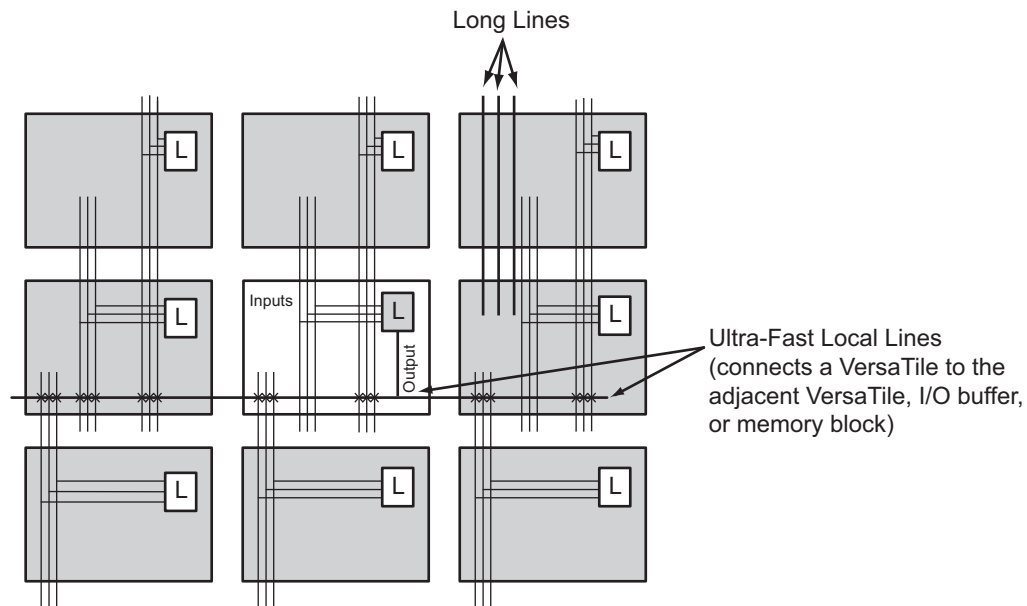
The routing structure of Fusion devices is designed to provide high performance through a flexible four-level hierarchy of routing resources: ultra-fast local resources; efficient long-line resources; high-speed very-long-line resources; and the high-performance VersaNet networks.

The ultra-fast local resources are dedicated lines that allow the output of each VersaTile to connect directly to every input of the eight surrounding VersaTiles (Figure 2-8). The exception to this is that the SET/CLR input of a VersaTile configured as a D-flip-flop is driven only by the VersaNet global network.

The efficient long-line resources provide routing for longer distances and higher-fanout connections. These resources vary in length (spanning one, two, or four VersaTiles), run both vertically and horizontally, and cover the entire Fusion device (Figure 2-9 on page 2-9). Each VersaTile can drive signals onto the efficient long-line resources, which can access every input of every VersaTile. Active buffers are inserted automatically by routing software to limit loading effects.

The high-speed very-long-line resources, which span the entire device with minimal delay, are used to route very long or high-fanout nets: length ± 12 VersaTiles in the vertical direction and length ± 16 in the horizontal direction from a given core VersaTile (Figure 2-10 on page 2-10). Very long lines in Fusion devices, like those in ProASIC3 devices, have been enhanced. This provides a significant performance boost for long-reach signals.

The high-performance VersaNet global networks are low-skew, high-fanout nets that are accessible from external pins or from internal logic (Figure 2-11 on page 2-11). These nets are typically used to distribute clocks, reset signals, and other high-fanout nets requiring minimum skew. The VersaNet networks are implemented as clock trees, and signals can be introduced at any junction. These can be employed hierarchically, with signals accessing every input on all VersaTiles.



Note: Input to the core cell for the D-flip-flop set and reset is only available via the VersaNet global network connection.

Figure 2-8 • Ultra-Fast Local Lines Connected to the Eight Nearest Neighbors

VersaNet Timing Characteristics

Global clock delays include the central rib delay, the spine delay, and the row delay. Delays do not include I/O input buffer clock delays, as these are dependent upon I/O standard, and the clock may be driven and conditioned internally by the CCC module. Table 2-5 and Table 2-6 present minimum and maximum global clock delays within the device. Minimum and maximum delays are measured with minimum and maximum loading, respectively.

Timing Characteristics

Table 2-5 • AFS1500 Global Resource Timing, Extended Temperature Case Conditions: $T_J = 100^\circ\text{C}$, $V_{CC} = 1.425\text{ V}$

Parameter	Description	-2		-1		Std.		Units
		Min. ¹	Max. ²	Min. ¹	Max. ²	Min. ¹	Max. ²	
t_{RCKL}	Input Low Delay for Global Clock	1.59	1.81	1.81	2.06	2.12	2.43	ns
t_{RCKH}	Input High Delay for Global Clock	1.59	1.86	1.81	2.12	2.13	2.49	ns
t_{RCKMPWH}	Minimum Pulse Width High for Global Clock	0.80		0.91		1.07		ns
t_{RCKMPWL}	Minimum Pulse Width Low for Global Clock	0.95		1.08		1.27		ns
t_{RCKSW}	Maximum Skew for Global Clock		0.27		0.31		0.36	ns

Notes:

1. Value reflects minimum load. The delay is measured from the CCC output to the clock pin of a sequential element located in a lightly loaded row (single element is connected to the global net).
2. Value reflects maximum load. The delay is measured on the clock pin of the farthest sequential element located in a fully loaded row (all available flip-flops are connected to the global net in the row).
3. For the derating values at specific junction temperature and voltage supply levels, refer to Table 3-7 on page 3-10.

Table 2-6 • AFS600 Global Resource Timing, Extended Temperature Case Conditions: $T_J = 100^\circ\text{C}$, $V_{CC} = 1.425\text{ V}$

Parameter	Description	-2		-1		Std.		Units
		Min. ¹	Max. ²	Min. ¹	Max. ²	Min. ¹	Max. ²	
t_{RCKL}	Input Low Delay for Global Clock	1.31	1.55	1.49	1.76	1.76	2.08	ns
t_{RCKH}	Input High Delay for Global Clock	1.31	1.59	1.49	1.81	1.75	2.13	ns
t_{RCKMPWH}	Minimum Pulse Width High for Global Clock	0.80		0.91		1.07		ns
t_{RCKMPWL}	Minimum Pulse Width Low for Global Clock	0.95		1.08		1.27		ns
t_{RCKSW}	Maximum Skew for Global Clock		0.28		0.32		0.38	ns

Notes:

1. Value reflects minimum load. The delay is measured from the CCC output to the clock pin of a sequential element located in a lightly loaded row (single element is connected to the global net).
2. Value reflects maximum load. The delay is measured on the clock pin of the farthest sequential element located in a fully loaded row (all available flip-flops are connected to the global net in the row).
3. For the derating values at specific junction temperature and voltage supply levels, refer to Table 3-7 on page 3-10.

Clock Conditioning Circuits

In Fusion devices, the CCCs are used to implement frequency division, frequency multiplication, phase shifting, and delay operations.

The CCCs are available in six chip locations—each of the four chip corners and the middle of the east and west chip sides.

Each CCC can implement up to three independent global buffers (with or without programmable delay), or a PLL function (programmable frequency division/multiplication, phase shift, and delays) with up to three global outputs. Unused global outputs of a PLL can be used to implement independent global buffers, up to a maximum of three global outputs for a given CCC.

A global buffer can be placed in any of the three global locations (CLKA-GLA, CLKB-GLB, and CLKC-GLC) of a given CCC.

A PLL macro uses the CLKA CCC input to drive its reference clock. It uses the GLA and, optionally, the GLB and GLC global outputs to drive the global networks. A PLL macro can also drive the YB and YC regular core outputs. The GLB (or GLC) global output cannot be reused if the YB (or YC) output is used (Figure 2-19). Refer to the "PLL Macro" section on page 2-27 for more information.

Each global buffer, as well as the PLL reference clock, can be driven from one of the following:

- 3 dedicated single-ended I/Os using a hardwired connection
- 2 dedicated differential I/Os using a hardwired connection
- The FPGA core

The CCC block is fully configurable, either via flash configuration bits set in the programming bitstream or through an asynchronous interface. This asynchronous interface is dynamically accessible from inside the Fusion device to permit changes of parameters (such as divide ratios) during device operation. To increase the versatility and flexibility of the clock conditioning system, the CCC configuration is determined either by the user during the design process, with configuration data being stored in flash memory as part of the device programming procedure, or by writing data into a dedicated shift register during normal device operation. This latter mode allows the user to dynamically reconfigure the CCC without the need for core programming. The shift register is accessed through a simple serial interface. Refer to the "UJTAG Applications in Microsemi's Low-Power Flash Devices" chapter of the *Fusion FPGA Fabric User's Guide* and the "CCC and PLL Characteristics" section on page 2-28 for more information.

The NGMUX macro is simplified to show the two clock options that have been selected by the GLMUXCFG[1:0] bits. Figure 2-25 illustrates the NGMUX macro. During design, the two clock sources are connected to CLK0 and CLK1 and are controlled by GLMUXSEL[1:0] to determine which signal is to be passed through the MUX.

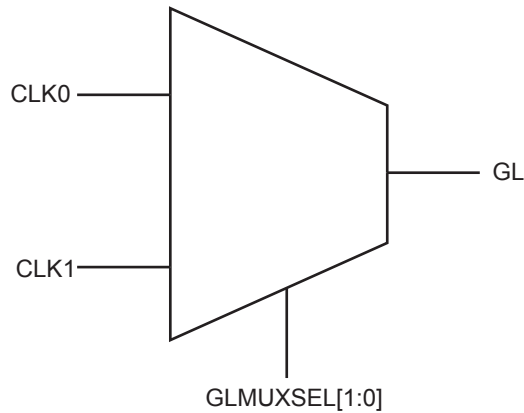


Figure 2-25 • NGMUX Macro

The sequence of switching between two clock sources (from CLK0 to CLK1) is as follows (Figure 2-26):

- GLMUXSEL[1:0] transitions to initiate a switch.
- GL drives one last complete CLK0 positive pulse (i.e., one rising edge followed by one falling edge).
- From that point, GL stays Low until the second rising edge of CLK1 occurs.
- At the second CLK1 rising edge, GL will begin to continuously deliver the CLK1 signal.
- Minimum $t_{sw} = 0.05$ ns at 25°C (typical conditions)

For examples of NGMUX operation, refer to the *Fusion FPGA Fabric User's Guide*.

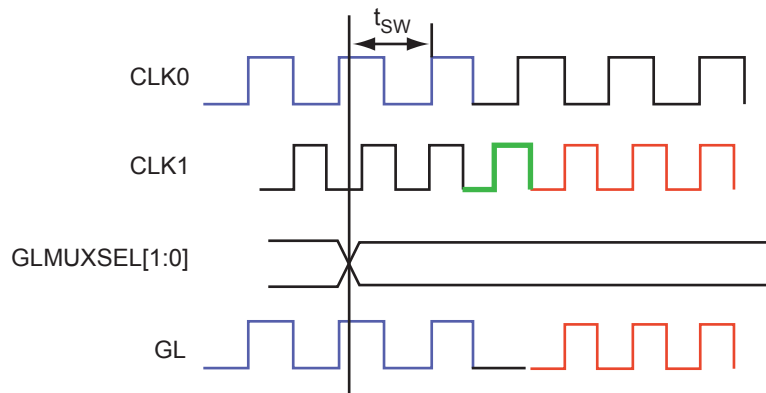


Figure 2-26 • NGMUX Waveform

Table 2-15 • RTC Control/Status Register

Bit	Name	Description	Default Value
7	rtc_rst	RTC Reset 1 – Resets the RTC 0 – Deassert reset on after two ACM_CLK cycle.	
6	cntr_en	Counter Enable 1 – Enables the counter; rtc_rst must be deasserted as well. First counter increments after 64 RTCCLK positive edges. 0 – Disables the crystal prescaler but does not reset the counter value. Counter value can only be updated when the counter is disabled.	0
5	vr_en_mat	Voltage Regulator Enable on Match 1 – Enables RTCMATCH and RTCPSMMATCH to output 1 when the counter value equals the Match Register value. This enables the 1.5 V voltage regulator when RTCPSMMATCH connects to the RTCPSMMATCH signal in VRPSM. 0 – RTCMATCH and RTCPSMMATCH output 0 at all times.	0
4:3	xt_mode[1:0]	Crystal Mode Controls RTCXTLMODE[1:0]. Connects to RTC_MODE signal in XTLOSC. XTL_MODE uses this value when xtal_en is 1. See the "Crystal Oscillator" section on page 2-18 for mode configuration.	00
2	rst_cnt_omat	Reset Counter on Match 1 – Enables the sync clear of the counter when the counter value equals the Match Register value. The counter clears on the rising edge of the clock. If all the Match Registers are set to 0, the clear is disabled. 0 – Counter increments indefinitely	0
1	rstb_cnt	Counter Reset, active Low 0 – Resets the 40-bit counter value	0
0	xtal_en	Crystal Enable Controls RTCXTLSEL. Connects to SELMODE signal in XTLOSC. 0 – XTLOSC enables control by FPGA_EN; xt_mode is not used. Sleep mode requires this bit to equal 0. 1 – Enables XTLOSC, XTL_MODE control by xt_mode Standby mode requires this bit to be set to 1. See the "Crystal Oscillator" section on page 2-18 for further details on SELMODE configuration.	0

Voltage Regulator and Power System Monitor (VRPSM)

The VRPSM macro controls the power-up state of the FPGA. The power-up bar (PUB) pin can turn on the voltage regulator when set to 0. TRST can enable the voltage regulator when deasserted, allowing the FPGA to power-up when user want access to JTAG ports. The inputs VRINITSTATE and RTCPSMMATCH come from the flash bits and RTC, and can also power up the FPGA

The following error indications are possible for Read operations:

1. STATUS = '01' when a single-bit data error was detected and corrected within the block addressed.
2. STATUS = '10' when a double-bit error was detected in the block addressed (note that the error is uncorrected).

In addition to data reads, users can read the status of any page in the FB by asserting PAGESTATUS along with REN. The format of the data returned by a page status read is shown in [Table 2-22](#), and the definition of the page status bits is shown in [Table 2-23](#).

Table 2-22 • Page Status Read Data Format

31	8	7	4	3	2	1	0
Write Count		Reserved		Over Threshold	Read Protected	Write Protected	Overwrite Protected

Table 2-23 • Page Status Bit Definition

Page Status Bit(s)	Definition
31–8	The number of times the page addressed has been programmed/erased
7–4	Reserved; read as 0
3	Over Threshold indicator (see the " Program Operation " section on page 2-46)
2	Read Protected; read protect bit for page, which is set via the JTAG interface and only affects JTAG operations. This bit can be overridden by using the correct user key value.
1	Write Protected; write protect bit for page, which is set via the JTAG interface and only affects JTAG operations. This bit can be overridden by using the correct user key value.
0	Overwrite Protected; designates that the user has set the OVERWRITEPROTECT bit on the interface while doing a Program operation. The page cannot be written without first performing an Unprotect Page operation.

FlashROM Characteristics

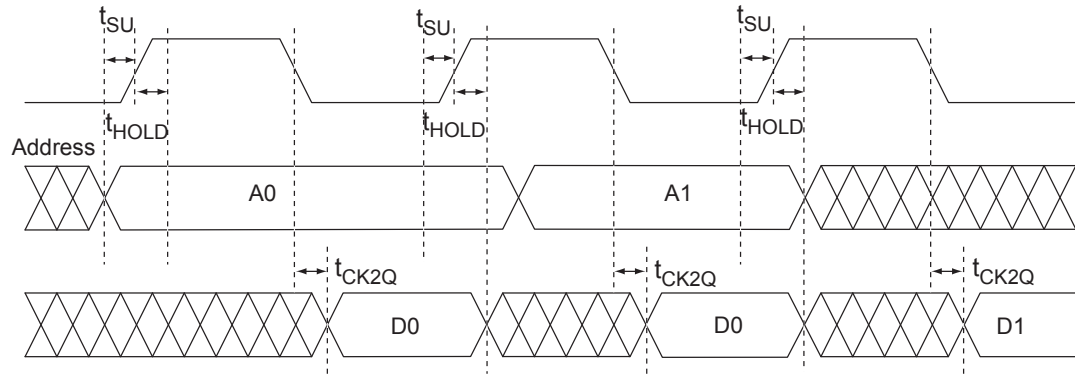


Figure 2-46 • FlashROM Timing Diagram

Table 2-25 • FlashROM Access Time, Extended Temperature Conditions: $T_J = 100^\circ\text{C}$, Worst-Case $V_{CC} = 1.425\text{ V}$

Parameter	Description	-2	-1	Std.	Units
t_{SU}	Address Setup Time	0.55	0.63	0.74	ns
t_{HOLD}	Address Hold Time	0.00	0.00	0.00	ns
t_{CK2Q}	Clock to Out	16.73	19.06	22.41	ns
FMAX	Maximum Clock frequency	40.00	40.00	40.00	MHz

FIFO Characteristics
Timing Waveforms

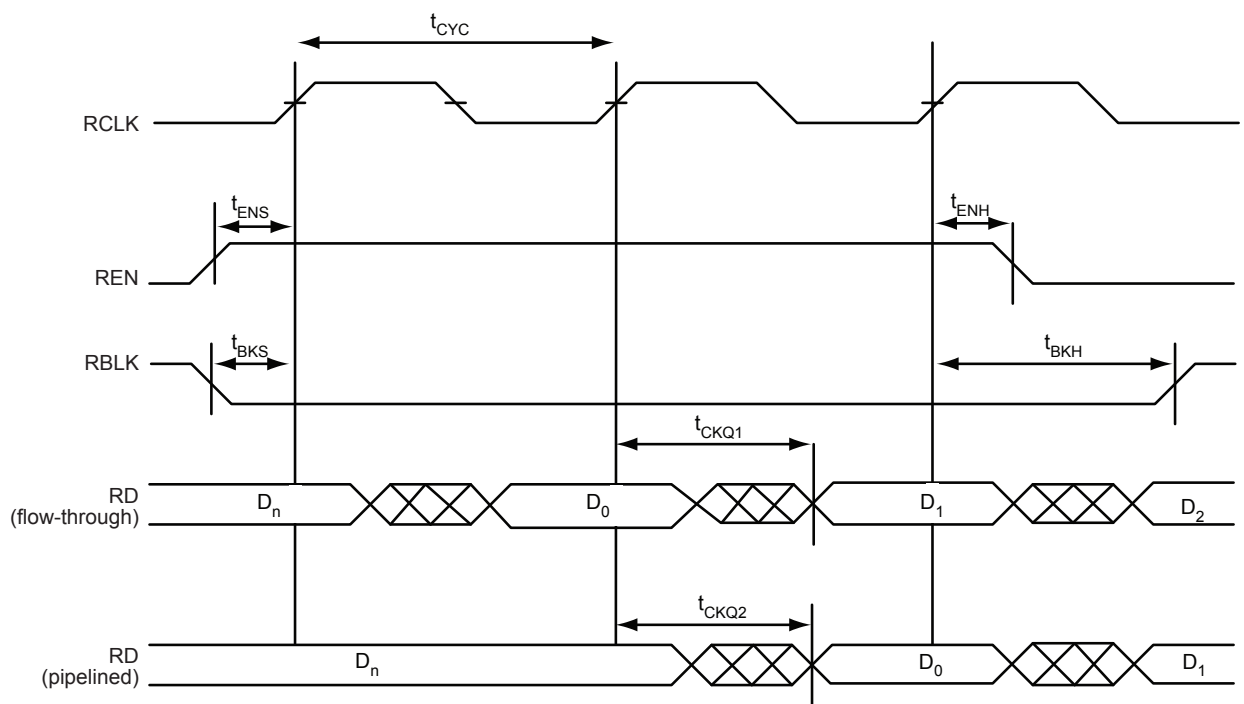


Figure 2-56 • FIFO Read

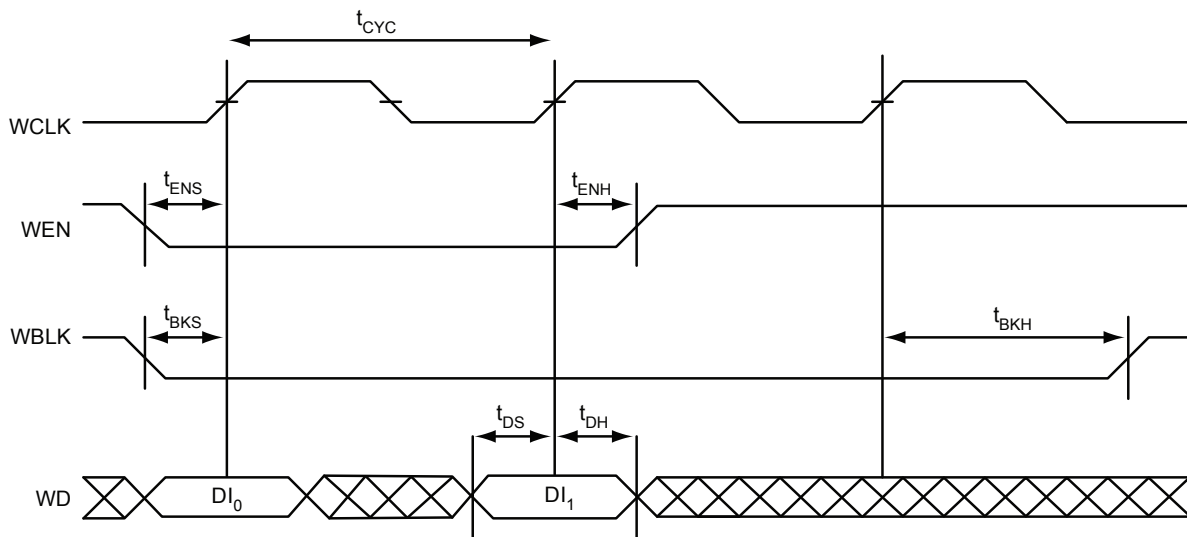


Figure 2-57 • FIFO Write

Direct Digital Input

The AV, AC, and AT pads can also be configured as high-voltage digital inputs (Figure 2-68). As these pads are 12 V-tolerant, the digital input can also be up to 12 V. However, the frequency at which these pads can operate is limited to 10 MHz.

To enable one of these analog input pads to operate as a digital input, its corresponding Digital Input Enable (DENAx_y) pin on the Analog Block must be pulled High, where x is either V, C, or T (for AV, AC, or AT pads, respectively) and y is in the range 0 to 9, corresponding to the appropriate Analog Quad.

When the pad is configured as a digital input, the signal will come out of the Analog Block macro on the appropriate DAXOUT_y pin, where x represents the pad type (V for AV pad, C for AC pad, or T for AT pad) and y represents the appropriate Analog Quad number. Example: If the AT pad in Analog Quad 5 is configured as a digital input, it will come out on the DATOUT5 pin of the Analog Block macro.

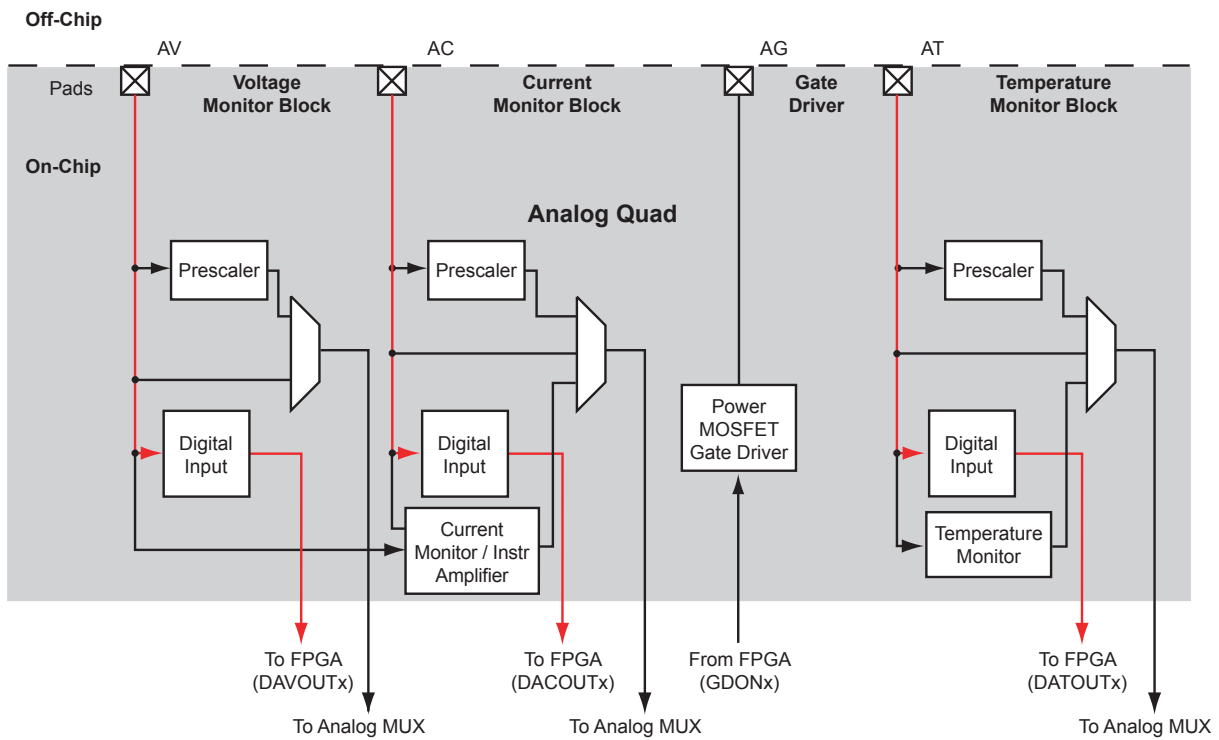


Figure 2-68 • Analog Quad Direct Digital Input Configuration

C_{GS} is not a fixed capacitance but, depending on the circuitry connected to its drain terminal, can vary significantly during the course of a turn-on or turn-off transient. Thus, EQ 6 on page 2-90 can only be used for a first-order estimate of the switching speed of the external MOSFET.

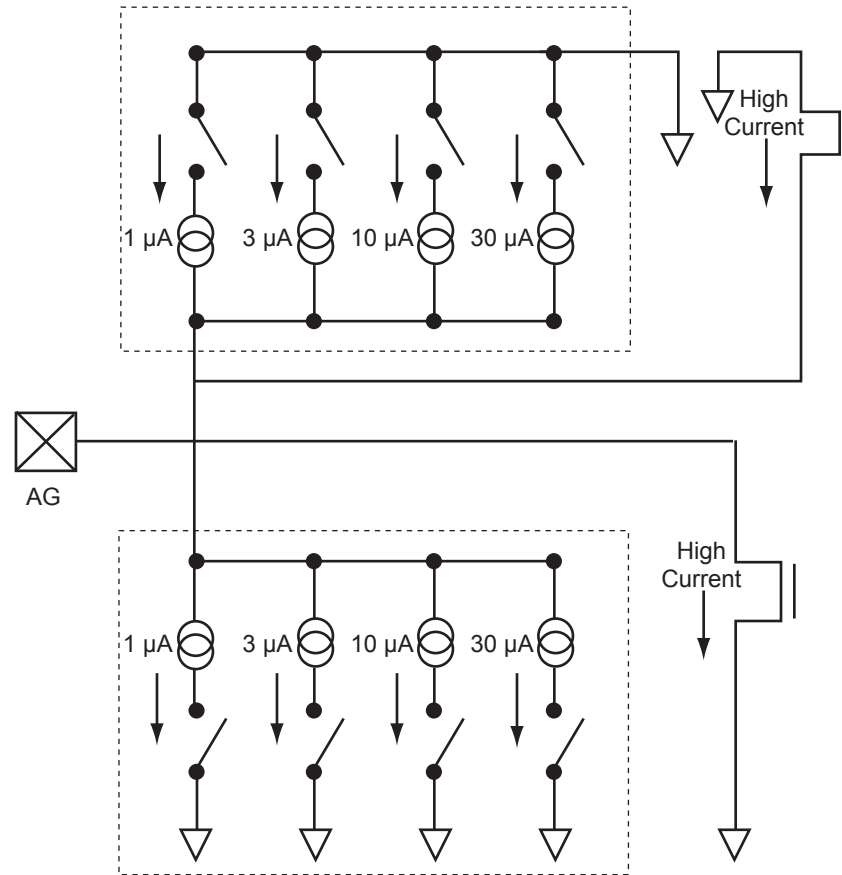


Figure 2-74 • Gate Driver Example

Table 2-39 • Analog MUX Channels (continued)

Analog MUX Channel	Signal	Analog Quad Number
16	AV5	Analog Quad 5
17	AC5	
18	AT5	
19	AV6	Analog Quad 6
20	AC6	
21	AT6	
22	AV7	Analog Quad 7
23	AC7	
24	AT7	
25	AV8	Analog Quad 8
26	AC8	
27	AT8	
28	AV9	Analog Quad 9
29	AC9	
30	AT9	
31	Internal temperature monitor	

The ADC can be powered down independently of the FPGA core, as an additional control or for power-saving considerations, via the PWRDWN pin of the Analog Block. The PWRDWN pin controls only the comparators in the ADC.

ADC Modes

The Fusion ADC can be configured to operate in 8-, 10-, or 12-bit modes, power-down after conversion, and dynamic calibration. This is controlled by MODE[3:0], as defined in Table 2-40.

The output of the ADC is the RESULT[11:0] signal. In 8-bit mode, the Most Significant 8 Bits RESULT[11:4] are used as the ADC value and the Least Significant 4 Bits RESULT[3:0] are logical '0's. In 10-bit mode, RESULT[11:2] are used the ADC value and RESULT[1:0] are logical 0s.

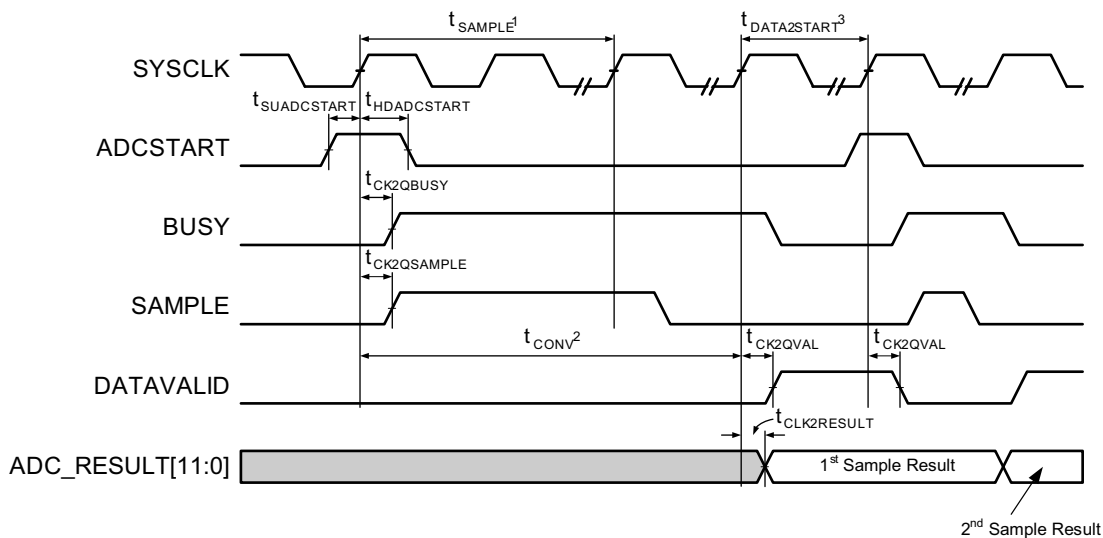
Table 2-40 • Mode Bits Function

Name	Bits	Function
MODE	3	0 – Internal calibration after every conversion; two ADCCLK cycles are used after the conversion. 1 – No calibration after every conversion
MODE	2	0 – Power-down after conversion 1 – No Power-down after conversion
MODE	1:0	00 – 10-bit 01 – 12-bit 10 – 8-bit 11 – Unused

Integrated Voltage Reference

The Fusion device has an integrated on-chip 2.56 V reference voltage for the ADC. The value of this reference voltage was chosen to make the prescaling and postscaling factors for the prescaler blocks change in a binary fashion. However, if desired, an external reference voltage of up to 3.3 V can be

Standard Conversion

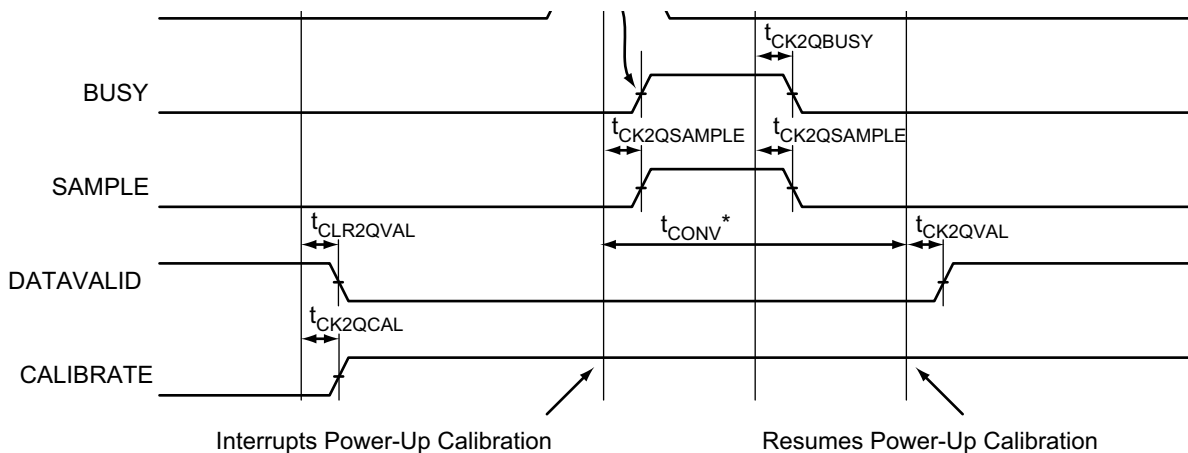


Notes:

1. Refer to EQ 20 on page 2-108 for the calculation on the sample time, t_{SAMPLE} .
2. See EQ 23 on page 2-109 for calculation on the conversion time, t_{CONV} .
3. Minimum time to issue an ADCSTART after DATAVALID is 1 SYSCLK period

Figure 2-90 • Standard Conversion Status Signal Timing Diagram

Intra-Conversion



Note: t_{CONV}^* represents the conversion time of the second conversion. See EQ 23 on page 2-109 for calculation of the conversion time, t_{CONV} .

Figure 2-91 • Intra-Conversion Timing Diagram

Table 2-50 • Electrical Characteristics (continued)

Parameter	Description	Condition	Min.	Typ.	Max.	Units
Temperature Monitor						
	Resolution			1		°C
	Accuracy			5	± 10	°C
VMPWT	Strobe	Minimum Pulse Width	10			µs
Analog Input as a Digital Input						
VIND	Input voltage		-0.2		AVDD + 0.2	V
VHYSIN	Hysteresis			0.3		V
VIHDIN	Input High			1.2		V
VILDIN	Input Low			0.9		V
VMPWDIN	Minimum pulse width		100			nS
I _{STBDIN}	Standby current				20	nA
I _{DYNDIN}	Dynamic current				20	µA
t _{INDIN}	Input delay			10		nS
Analog Output Pad (G pad)						
VG	Voltage Range		-12		12	V
IG	Minimum output current drive	High current mode at 1.0 V		25		mA
		Low current mode—1 µA		1		µA
		Low current mode—3 µA		3		µA
		Low current mode—10 µA		10		µA
		Low current mode—30 µA		30		µA
IOFFG	Maximum Off Current			100		µA

Notes:

1. The sample rate is time-shared among active analog inputs.
2. The input voltage range for the temperature monitor block prescaler is 0 to 12 V.
3. VRSM is the maximum voltage drop across the current sense resistor.

Table 2-96 • I/O Short Currents IOSH/IOSL

	Drive Strength	IOSH (mA)*	IOSL (mA)*
Applicable to Pro I/O Banks			
3.3 V LVTTTL / 3.3 V LVCMOS	4 mA	25	27
	8 mA	51	54
	12 mA	103	109
	16 mA	132	127
	24 mA	268	181
2.5 V LVCMOS	4 mA	16	18
	8 mA	32	37
	12 mA	65	74
	16 mA	83	87
	24 mA	169	124
1.8 V LVCMOS	2 mA	9	11
	4 mA	17	22
	6 mA	35	44
	8 mA	45	51
	12 mA	91	74
	16 mA	91	74
1.5 V LVCMOS	2 mA	13	16
	4 mA	25	33
	6 mA	32	39
	8 mA	66	55
	12 mA	66	55
Applicable to Advanced I/O Banks			
3.3 V LVTTTL / 3.3 V LVCMOS	2 mA	25	27
	4 mA	25	27
	6 mA	51	54
	8 mA	51	54
	12 mA	103	109
	16 mA	132	127
	24 mA	268	181
3.3 V LVCMOS	2 mA	25	27
	4 mA	25	27
	6 mA	51	54
	8 mA	51	54
	12 mA	103	109
	16 mA	132	127
	24 mA	268	181

Note: *T_J = 100°C

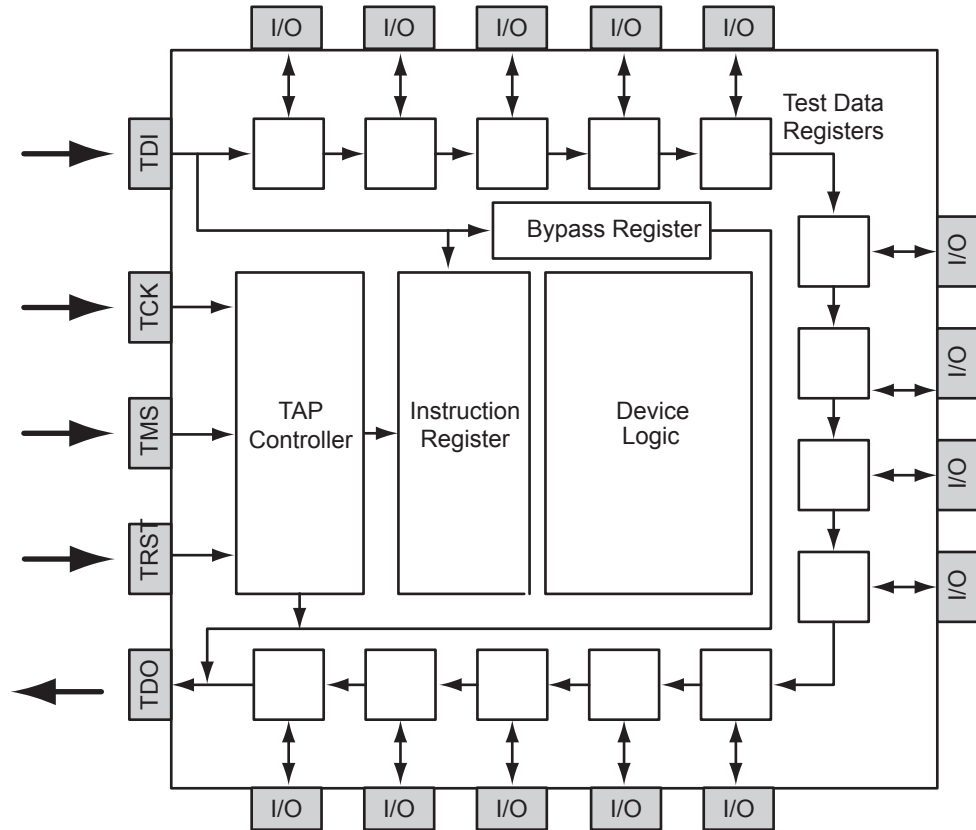


Figure 2-144 • Boundary Scan Chain in Fusion

Table 2-176 • Boundary Scan Opcodes

	Hex Opcode
EXTEST	00
HIGHZ	07
USERCODE	0E
SAMPLE/PRELOAD	01
IDCODE	0F
CLAMP	05
BYPASS	FF

Theta-JA

Junction-to-ambient thermal resistance (θ_{JA}) is determined under standard conditions specified by JEDEC (JESD-51), but it has little relevance in actual performance of the product. It should be used with caution but is useful for comparing the thermal performance of one package to another.

A sample calculation showing the maximum power dissipation allowed for the AFS600-FG484 package under forced convection of 1.0 m/s and 75°C ambient temperature is as follows:

$$\text{Maximum Power Allowed} = \frac{T_{J(\text{MAX})} - T_{A(\text{MAX})}}{\theta_{JA}}$$

EQ 4

where

$$\theta_{JA} = 19.00^\circ\text{C/W (taken from Table 3-6 on page 3-8).}$$

$$T_A = 75.00^\circ\text{C}$$

$$\text{Maximum Power Allowed} = \frac{100.00^\circ\text{C} - 75.00^\circ\text{C}}{19.00^\circ\text{C/W}} = 1.3 \text{ W}$$

EQ 5

The power consumption of a device can be calculated using the Microsemi power calculator. The device's power consumption must be lower than the calculated maximum power dissipation by the package. If the power consumption is higher than the device's maximum allowable power dissipation, a heat sink can be attached on top of the case, or the airflow inside the system must be increased.

Theta-JB

Junction-to-board thermal resistance (θ_{JB}) measures the ability of the package to dissipate heat from the surface of the chip to the PCB. As defined by the JEDEC (JESD-51) standard, the thermal resistance from junction to board uses an isothermal ring cold plate zone concept. The ring cold plate is simply a means to generate an isothermal boundary condition at the perimeter. The cold plate is mounted on a JEDEC standard board with a minimum distance of 5.0 mm away from the package edge.

Theta-JC

Junction-to-case thermal resistance (θ_{JC}) measures the ability of a device to dissipate heat from the surface of the chip to the top or bottom surface of the package. It is applicable for packages used with external heat sinks. Constant temperature is applied to the surface in consideration and acts as a boundary condition. This only applies to situations where all or nearly all of the heat is dissipated through the surface in consideration.

Calculation for Heat Sink

For example, in a design implemented in an AFS600-FG484 package with 2.5 m/s airflow, the power consumption value using the power calculator is 3.00 W. The user-dependent T_a and T_j are given as follows:

$$T_J = 100.00^\circ\text{C}$$

$$T_A = 70.00^\circ\text{C}$$

From the datasheet:

$$\theta_{JA} = 17.00^\circ\text{C/W}$$

$$\theta_{JC} = 8.28^\circ\text{C/W}$$

$$P = \frac{T_J - T_A}{\theta_{JA}} = \frac{100^\circ\text{C} - 70^\circ\text{C}}{17.00 \text{ W}} = 1.76 \text{ W}$$

EQ 6

FG484		
Pin Number	AFS600 Function	AFS1500 Function
A1	GND	GND
A2	VCC	NC
A3	GAA1/IO01PDB0V0	GAA1/IO01PDB0V0
A4	GAB0/IO02NDB0V0	GAB0/IO02NDB0V0
A5	GAB1/IO02PDB0V0	GAB1/IO02PDB0V0
A6	IO07NDB0V1	IO07NDB0V1
A7	IO07PDB0V1	IO07PDB0V1
A8	IO10PDB0V1	IO09PDB0V1
A9	IO14NDB0V1	IO13NDB0V2
A10	IO14PDB0V1	IO13PDB0V2
A11	IO17PDB1V0	IO24PDB1V0
A12	IO18PDB1V0	IO26PDB1V0
A13	IO19NDB1V0	IO27NDB1V1
A14	IO19PDB1V0	IO27PDB1V1
A15	IO24NDB1V1	IO35NDB1V2
A16	IO24PDB1V1	IO35PDB1V2
A17	GBC0/IO26NDB1V1	GBC0/IO40NDB1V2
A18	GBA0/IO28NDB1V1	GBA0/IO42NDB1V2
A19	IO29NDB1V1	IO43NDB1V2
A20	IO29PDB1V1	IO43PDB1V2
A21	VCC	NC
A22	GND	GND
AA1	VCC	NC
AA2	GND	GND
AA3	VCCIB4	VCCIB4
AA4	VCCIB4	VCCIB4
AA5	PCAP	PCAP
AA6	AG0	AG0
AA7	GND	GND
AA8	AG1	AG1
AA9	AG2	AG2
AA10	GND	GND
AA11	AG3	AG3
AA12	AG6	AG6
AA13	GND	GND

FG484		
Pin Number	AFS600 Function	AFS1500 Function
AA14	AG7	AG7
AA15	AG8	AG8
AA16	GND	GND
AA17	AG9	AG9
AA18	VAREF	VAREF
AA19	VCCIB2	VCCIB2
AA20	PTEM	PTEM
AA21	GND	GND
AA22	VCC	NC
AB1	GND	GND
AB2	VCC	NC
AB3	NC	IO94NSB4V0
AB4	GND	GND
AB5	VCC33N	VCC33N
AB6	AT0	AT0
AB7	ATRNT0	ATRNT0
AB8	AT1	AT1
AB9	AT2	AT2
AB10	ATRNT1	ATRNT1
AB11	AT3	AT3
AB12	AT6	AT6
AB13	ATRNT3	ATRNT3
AB14	AT7	AT7
AB15	AT8	AT8
AB16	ATRNT4	ATRNT4
AB17	AT9	AT9
AB18	VCC33A	VCC33A
AB19	GND	GND
AB20	NC	IO76NPB2V0
AB21	VCC	NC
AB22	GND	GND
B1	VCC	NC
B2	GND	GND
B3	GAA0/IO01NDB0V0	GAA0/IO01NDB0V0
B4	GND	GND